

---

# PixFoundation: Are We Heading in the Right Direction with Pixel-level Vision Foundation Models?

---

Mennatullah Siam<sup>1</sup>

## Abstract

Multiple works have emerged to push the boundaries on multi-modal large language models (MLLMs) towards pixel-level understanding. Such approaches have shown strong performance on benchmarks for referring expression segmentation and grounded conversation generation. The current trend in pixel-level MLLMs is to train with pixel-level grounding supervision on large-scale labelled data. However, we show that such MLLMs when evaluated on recent challenging vision centric benchmarks, exhibit a weak ability in visual question answering. Surprisingly, some of these methods even downgrade the grounding ability of MLLMs that were never trained with such supervision. In this work, we propose two novel challenging benchmarks and show that MLLMs without pixel-level grounding supervision can outperform the state of the art in such tasks when evaluating both the pixel-level grounding and visual question answering. We propose simple baselines to extract the grounding information that can be plugged into any MLLM, which we call as PixFoundation. More importantly, we study the research question of “When does grounding emerge in MLLMs that are not trained with pixel-level grounding supervision?” We show that grounding can coincide with object parts or location/appearance information. Code repository is at <https://github.com/MSiam/PixFoundation/>.

## 1. Introduction

There have been numerous advancements in pixel-level image and video understanding, including tasks such as image/video segmentation (Zhou et al., 2022; Minaee et al., 2021; Kirillov et al., 2023; Ravi et al., 2024), pixel-level vi-

<sup>1</sup>Department of Computer Science, University of British Columbia, Canada. Correspondence to: Mennatullah Siam <mennatullah.siam@ubc.ca>.

Under review.

Are pixel-level MLLMs heading in the right direction to improve VQA and grounding? proposing PixMMVP, PixCV-Bench benchmarks

Question: Are the butterfly's feet visible?



(a) Yes (b) No



(a) Yes (b) No



Corresponding Pixel-level Visual Grounding

When does grounding emerge in Multi-modal Large Language Models?

Instruction: Identify the butterfly's feet in the scene.

The butterfly's feet are visible in the scene, with one foot on the plant ...

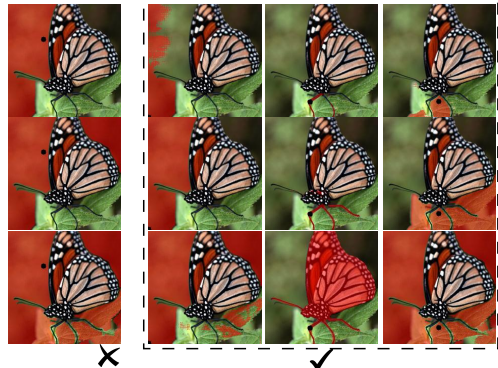


Figure 1. The two major research questions we explore: (i) the grounding ability of pixel-level MLLMs in challenging scenarios (first row), (ii) the ability of vanilla MLLMs to perform grounding and when does it emerge (second row). Second row shows the noun phrase and its corresponding segmentation mask, highlighted in red, extracted from Llava 1.5 (Liu et al., 2024) attention maps with three possible output masks to accommodate ambiguity in the point prompt, highlighted as a black dot.

sual grounding and reasoning (Rasheed et al., 2024; Lai et al., 2024), depth estimation (Yang et al., 2024) and tracking (Wang et al., 2023). The majority of these have been transformed with the emergence of foundation models (Bommasani et al., 2021), specifically multi-modal large language models (MLLMs) (Liu et al., 2023; Dai et al., 2023). Nonetheless, pixel-level MLLMs have shown degradation in their capabilities in chat performance (Lai et al., 2024). Recent models tried to address this gap (Zhang et al., 2024b;a), yet they relied on standard evaluation benchmarks overlooking the shortcomings of current MLLMs.

Recent efforts explored the shortcomings of MLLMs in vision centric benchmarks (Tong et al., 2024b;a). Such benchmarks focus on challenging visual patterns and tasks such as counting and relative positioning. Nonetheless, these benchmarks did not evaluate the recent pixel-level MLLMs. In this work we aim to provide challenging vision centric benchmarks that are dedicated to evaluate these models. Through these, we answer the first research question; “*Are the current pixel-level MLLMs trained with full grounding supervision heading in the right direction to improve both grounding and visual question answering (VQA) among other capabilities?*”. Our findings show that the majority of pixel-level MLLMs still fall short in such challenging setting. While evidently, some of these show superior performance in visual grounding, we show that MLLMs that were not trained with pixel-level grounding can have better performance without degrading their capabilities.

There have been recent works showing training-free open vocabulary segmentation emerging from vision language models (Wang et al., 2024; Luo et al., 2024; Hajimiri et al., 2025). Concurrent work has specifically explored emerging grounding in MLLMs (Cao et al., 2024). We are inspired by the previous work to establish a baseline on our proposed benchmarks. However, unlike their method we focus on the second research question of “*When does grounding emerge in MLLMs that are not trained with full grounding supervision?*”. Previous efforts studying emergent segmentation and/or grounding assumed correspondence with the specific language tokens (i.e., nouns or noun phrases) of the objects of interest. However, our work documents that emerging grounding in MLLMs does not necessarily coincide with the exact language tokens of the object. We show it mostly emerges in the last 40% of the output, and can coincide with concepts about object parts, position/location, color/appearance or context of these objects. Fig. 1 summarizes our two major research questions.

In summary, our contributions include: (i) Providing pixel-level segmentation annotations and referring expression of the object of interest in the question for two vision centric benchmarks (Tong et al., 2024a;b), which are PixMMVP and PixCV-Bench. (ii) Benchmarking recent efforts in pixel-level MLLMs where we show that they degrade VQA capabilities. More importantly, some of them lag in visual grounding with respect to simple techniques of extracting the segmentation from vanilla MLLMs, i.e., MLLMs that are not trained for pixel-level grounding. (iii) We provide a simple mechanism for extracting segmentation from vanilla MLLMs, with an understanding of when grounding emerges. Our mechanism uses the observation that grounding can emerge corresponding to different output tokens describing the object’s appearance or location, not necessarily the exact text of the object of interest. We call it PixFoundation, since it mines the foundation model for pixel-level understanding.

## 2. Related Work

**Pixel-level Vision Foundation Models.** There have been various vision foundation models released that were trained with supervision for the segmentation task (e.g., SAM, SAM 2.0) (Kirillov et al., 2023; Ravi et al., 2024). Orthogonal to this, some methods discussed the ability of vision foundation models such as CLIP and BLIP in image segmentation without any segmentation supervision (Luo et al., 2024; Hajimiri et al., 2025; Wang et al., 2024). Yet, they relied on earlier foundation models that did not incorporate the power of large language models. Combining large language models with vision has been extensively researched with pioneering works such as Llava (Liu et al., 2023;/ 2024) and instruct-BLIP (Dai et al., 2023). Multiple works afterwards focused on pixel-level visual grounding in these MLLMs with full supervision (Lai et al., 2024; Rasheed et al., 2024; Zhang et al., 2024a;b;a;b). However, these methods were lagging in their chat performance. Notably, pixel-level MLLMs were not evaluated on the challenging benchmarks that focused on the shortcomings of MLLMs (Tong et al., 2024b;a). Hence, it is still unclear if the pixel-level grounding supervision helped to improve their ability on these challenging tasks or not. In this work, we focus on the previous question to have a better understanding of their performance. Concurrent work, has shown that without pixel-level supervision there is an emerging ability to perform pixel-level grounding (Cao et al., 2024). We rely on this method as our baseline, but unlike previous works we provide an insight on when grounding emerges in such MLLMs.

### Benchmarking Multi-modal Large Language Models

There is an abundance of standard benchmarks used for evaluating MLLMs (e.g., MMU (Yue et al., 2024)) and their pixel-level counter parts (e.g., refCOCO/+g (Yu et al., 2016; Kazemzadeh et al., 2014)). These benchmarks have pushed the limits on MLLMs capabilities in terms of VQA and visual grounding. Nonetheless, there have been various works that discussed the shortcomings of MLLMs. In one of these works they discussed specifically CLIP (Radford et al., 2021), which is used in various MLLMs as the visual backbone. They proposed a benchmark, MMVP (Tong et al., 2024b), that is focused on the visual aspects within a VQA task designed on CLIP blind pairs. More recently, CV-Bench (Tong et al., 2024a) focused on two major tasks that are vision focused which are counting and relative positioning. Both were proposed to evaluate MLLMs that do not have the ability to generate segmentation output. Nonetheless, they still provide quite challenging scenarios that can act as a strong benchmark for the pixel-level MLLMs counterpart. In this work, we extend these two benchmarks to augment it with pixel-level annotations and referring expressions that correspond to the object of interest within their VQA task. These help to understand if failures occurring in these benchmarks stem from grounding or other reasons.

**Prompt:** Based on the image, is the following statement correct: We cannot see the window on the school bus?  
 (a) Correct (b) Incorrect



Answer: It is [SEG].



Answer: It is [SEG].



Answer: It is [SEG].



Answer: It is [SEG].



Answer: ...the statement is incorrect. The image shows a school bus with a stop sign...



Answer: (b) Incorrect

**LISA**

**GLAMM**

**OMG-Llava**

Figure 2. First shortcoming of pixel-level MLLMs is the degraded performance in visual question answering. The Predicted segmentation masks corresponding to the [SEG] token/s are highlighted in red.

### 3. Method and Benchmarks

In this section, we describe our two benchmarks and probing techniques for pixel-level MLLMs and MLLMs that were not trained with pixel-level grounding supervision.

#### 3.1. Benchmarks

**PixMMVP benchmark:** We build upon the recently released MMVP (Tong et al., 2024b) which identified clip blind pairs and used them to build a challenging benchmark with the corresponding questions and choices for 300 images. We augment the aforementioned dataset and manually annotate each question with the corresponding object of interest referring expression, e.g. an elderly person or the butterfly’s feet. There are seven questions only that are not designed to inquire about a specific object in the scene, which are excluded. Examples include questions inquiring on the view direction of the camera which are not tied to a specific entity. Our manual referring expression annotations are as fine-grained as possible. These expressions correspond to what needs to be grounded in the image to answer the question. Afterwards, we manually label these objects of interest with polygonal annotations using the VGG annotator (Dutta et al., 2016).

**PixCV-Bench benchmark:** For this benchmark we build upon the 2D component of the recently released CV-Bench (Tong et al., 2024a). We specifically select the 2D component, since they are sourced from segmentation datasets (i.e., ADE20K (Zhou et al., 2017) and COCO (Lin et al., 2014)), which can be used in our proposed benchmark. However, the publicly released CV-Bench does not identify the objects in question and their corresponding segmentation. As such we use GPT-4o to parse the questions and identify the objects of interest automatically, followed by manual inspection and correction. Specifically, we collect the classes in each image from the corresponding dataset and construct a list of class choices “1. <CLS1>, 2. <CLS2>,

...”. Then we prompt GPT-4o with the following, “*Provide number only as an answer. Identify the objects of interest in the following question: <QUESTION> ? 1. <CLS1>, 2. <CLS2>, ...*”. This provides us with the categories per question that highlights the objects of interest. While seemingly these are categorical annotations not referring expressions, certain scenarios in CV-Bench are different. Specifically, in the relative positioning task all the questions that include an object highlighted by a red box in the image are annotated with the referring expression, “(annotated by the red box)”, beyond simple categorical annotations.

Afterwards, we use the selected categories from GPT-4o to retrieve the corresponding segmentation mask/s per image. Furthermore, we use a custom annotation tool to manually filter the objects in the question, e.g. selecting only the object mask annotated by the red box when referred to it and filtering out the other instances for that same class. Another example that needs manual filtration when the class in question is a broader category than what is inquired upon, e.g., “Pendant Lamp” which is under the category of “Lamp” in ADE20K. In such a case we need to filter out the masks of other types such as “Table Lamp”. Moreover, we identified missing annotations in rare occasions that required additional intervention. Examples include transparent objects such as wine glasses which were partially occluded, yet the ground-truth answer of the CV-Bench question included that object in the count. As such, we use VGG annotator for these missing annotations that were not part of the original segmentation masks. We provide the final PixCV-Bench with referring expressions and their segmentation annotations that can be used to evaluate the grounding ability in relation to the original VQA task. Appendix A provides visual examples from our benchmarks.

#### 3.2. A Pixel-level MLLMs Study

We utilize the two proposed benchmarks, PixMMVP and PixCV-Bench, to evaluate how the current trend in pixel-



Figure 3. Second shortcoming of pixel-level MLLMs is the degraded performance in pixel-level visual grounding in certain models. The predicted segmentation is highlighted in red.

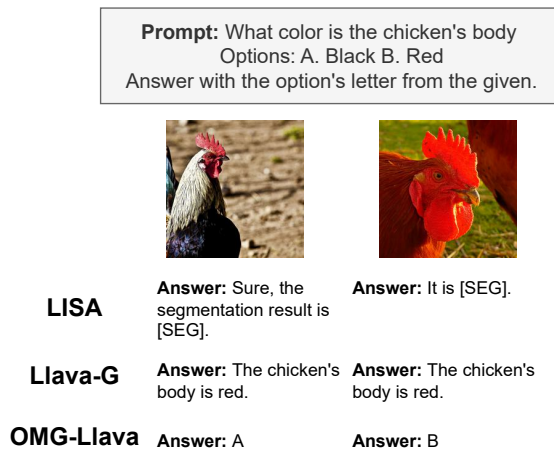


Figure 4. Third shortcoming of pixel-level MLLMs is the degraded performance in instruction following, where the question is instructing the model to generate one letter from the options.

level MLLMs that relies on training with grounding supervision perform in such challenging tasks. Furthermore, we inspect the failures of these pixel-level MLLMs and explore simple approaches to pixel-level understanding from MLLMs that overcome the previous shortcomings.

**Pixel-level MLLMs Shortcomings.** We highlight the failures for the current state-of-the-art pixel-level MLLMs through three probing techniques. First, we highlight the degraded performance in VQA from most of the pixel-level MLLMs that are trained with pixel-level grounding supervision. We use for the first prompt “ $<IMG><QUESTION>? <OPTION1> <OPTION2>...</$ ”, as shown in Figure 2. Certain pixel-level MLLMs tend to answer the aforementioned question while outputting a corresponding segmentation mask/s for the objects of interest. Notably, the

worst two models in this task, LISA (Lai et al., 2024) and GLAMM (Rasheed et al., 2024), are not able to provide an answer and rather refer to a segmentation mask. On the other hand, OMG-Llava (Zhang et al., 2024b) shows better ability in visual question answering.

The second shortcoming we discuss is their degraded ability to visually ground objects. Surprisingly, although they were trained with pixel-level grounding supervision, not all of these models show superior grounding performance. Figure 3 shows the second prompt to generate a segmentation mask for the ground-truth referring expression. The purpose of this probing is to understand whether the failure in these models is purely on the VQA task, or its inability to ground the objects of interest in the corresponding question or both. Figure 3 shows the worst two models in this aspect, which are GLAMM, the region captioning variant, and Llava-G. Both fail to segment the specific object in question, while OMG-Llava shows better performance in grounding.

Third, we highlight another shortcoming, where these MLLMs exhibit degraded ability to follow instructions. In order to probe this, we use the following prompt: “ $<IMG><QUESTION>? a.<OPTION1> b.<OPTION2>...</$  Answer with the option's letter from the given.” Figure 4 shows an example with the answers from the worst two models in this aspect which are LISA (Lai et al., 2024) and Llava-G (Zhang et al., 2024a). Both are incapable of following the instruction, yet Llava-G tries to tackle the question unlike LISA. On the other hand, OMG-Llava shows better ability to follow the instruction and answer the question.

**Baselines and upper bounds.** In addition to evaluating state-of-the-art pixel-level MLLMs, we propose two baselines and one upper bound. The first of which is inspired by a concurrent work (Cao et al., 2024) that identified the emergent grounding in multi-modal large language models without the need for any pixel-level grounding supervision.

Specifically, we use their attend and segment meta architecture as one of our baselines. However, we are the first to discuss when does such grounding emerge in these models. We identify an interesting connection between the identified output tokens and the output grounding from the attention maps that gives insights on how these models reason.

The attend and segment meta-architecture extracts the raw attention map for the  $i^{th}$  output token,  $A_i \in [0, 1]^{n_{layer} \times n_{head} \times (x+hw+y+i-1)}$ , where  $n_{layer}, n_{head}$  are the number of layers and heads, resp. Then,  $x, y$  are the number of input language tokens before and after the visual tokens respectively, while  $hw$  are the height and width of the input image. Only the attention corresponding to the visual tokens of length  $hw$  are used, and these attention maps are averaged across the layers and heads, resulting in  $\bar{A}_i \in [0, 1]^{h \times w}$ . This is further normalized across all the output,  $\tilde{A}_i = \bar{A}_i - \frac{1}{N} \sum_{j=1}^N \bar{A}_j$  for  $N$  output tokens. The attend and segment depends on using spaCy natural language processing tool (Honnibal et al., 2020) to identify the noun phrases and associate them to the ground-truth referring expressions. Thus, the spaCy embeddings closest to the ground-truth expression are used in the mask selection. This is followed by extracting the maximum attention point to feed into SAM (Kirillov et al., 2023) as a point prompt.

For our baseline and upper bound, we build upon the previous pipeline and build an *oracle* upper bound and an *automatic* baseline. We introduce two main modifications to account for our observation that the correct grounding can occur with different output tokens describing the object not necessarily aligning with the exact ground-truth expression. The first modification is to go through all the potential output tokens without relying on spaCy embeddings. In the *oracle* we rely on the ground-truth mask to select the correct token and its corresponding attention map with highest intersection over union as an upper bound. The *automatic* baseline uses a simple but powerful mechanism where we overlay the predicted masks on the original image to highlight the potential object of interest. This is followed by feeding these images to a multi-modal LLM inquiring on which is best in highlighting this object. Specifically, we use the following prompt “*Select the image that has <EXPR> best highlighted in red color than the others? Answer with a number from 1 to <N> and mention the number only. <IMG>*”, where  $<\text{EXPR}>$  and  $<\text{IMG}>$  are the ground-truth expression and the image tokens respectively. In our experiments we rely on the open source Cambrian-1(8B) (Tong et al., 2024a) model in our automatic baseline for the mask selection. The second modification since SAM has a good understanding of point prompting ambiguity, we process three potential output masks for each prompt instead of a single one. This enables us to utilize the power of SAM in identifying fine-grained objects and referring expressions that tends to surpass what other MLLMs do,

even those trained with pixel-level grounding supervision.

## 4. Experiments

### 4.1. Experimental Setup

**Evaluation benchmarks, protocols and metrics.** PixM-MVP is composed of 300 images paired with questions, choices, referring expressions and segmentation masks, while PixCV-Bench has 1,438 images with their corresponding annotations similarly. On each benchmark we evaluate the VQA and visual grounding capabilities following three probing techniques and reporting their metrics. The first probing is to evaluate the VQA ability, where the accuracy is computed using GPT-4o following (Tong et al., 2024b) as,  $\mathcal{A}\dagger$ . If the model generates a segmentation without explicitly asking it to, it is evaluated with respect to the ground-truth referring segmentation in terms of mean intersection over union as,  $\mathcal{M}\dagger$ . The second probing prompts the model to identify the referred expression then evaluates the mean intersection over union reported as,  $\mathcal{M}$ . The third probing following (Tong et al., 2024a) instructs the model to generate a single option letter and evaluate the accuracy directly without GPT-4o, reported as,  $\mathcal{A}$ . There is a need for the first probing since some of the recent pixel-level MLLMs face challenges in following instructions. We evaluate the score of each model,  $\mathcal{S}$ , which is the harmonic mean across the maximum of both pixel-level visual grounding and VQA,

$$\mathcal{S} = \frac{2}{\frac{1}{\max(\mathcal{A}, \mathcal{A}\dagger)} + \frac{1}{\max(\mathcal{M}, \mathcal{M}\dagger)}}. \quad (1)$$

We mainly focus on evaluating four state-of-the-art pixel-level MLLMs; LISA (Lai et al., 2024), GLAMM (Rasheed et al., 2024), OMG-Llava (Zhang et al., 2024b) and Llava-G (Zhang et al., 2024a). For GLAMM we use two variants; the original model (GLAMM) and the one fine-tuned for region-level captioning, (GLAMM-RegCap). We use Hugging Face for these models weights, refer to Appendix A.

**Baselines and upper bound implementation details.** We evaluate: (i) the attend and segment (a+s), (ii) the *oracle* selection relying on the highest intersection over union in selecting the correctly predicted masks (PixFoundation $\dagger$ ), and (iii) the *automatic* selection, (PixFoundation). These are implemented on top of three base MLLMs which are, Llava 1.5 (7B, 13B) (Liu et al., 2024) and Cambrian-1(8B) (Tong et al., 2024a). The automatic selection is implemented using the Cambrian-1 (8B) model, yet it can be further improved using GPT-4o, refer to Appendix A for more details.

### 4.2. Are the current pixel-level MLLMs heading in the right direction?

In order to answer this, we evaluate each of these pixel-level MLLMs capability in VQA in challenging tasks. Addition-

Method	PixGr. Train	MMVP & PixMMVP				$\mathcal{S}$
		$\mathcal{A}^\dagger$	$\mathcal{A}$	$\mathcal{M}^\dagger$	$\mathcal{M}$	
Llava 1.5 (7B) (Liu et al., 2023/)	X	<b>28.7</b>	<b>28.0</b>	-	-	-
Llava 1.5 (13B) (Liu et al., 2023/)	X	<b>39.3</b>	<b>30.0</b>	-	-	-
Cambrian (8B)* (Tong et al., 2024a)	X	<b>52.0</b>	<b>52.0</b>	-	-	-
OMG Llava (7B) (Zhang et al., 2024b)	✓	12.0	12.0	17.8	38.0	18.2
GLAMM (7B) (Rasheed et al., 2024)	✓	1.3	2.7	<b>31.5</b>	<b>47.4</b>	5.1
GLAMM - RegCap (7B) (Rasheed et al., 2024)	✓	12.7	6.7	14.5	18.6	15.1
LISA (7B) (Lai et al., 2024)	✓	7.3	-	18.1	42.9	12.5
Llava-G (7B) (Zhang et al., 2024a)	✓	9.3	-	17.8	13.5	12.2
Llava 1.5 (7B) + (a+s) (Cao et al., 2024)	X	<b>28.7</b>	<b>28.0</b>	11.1	11.2	16.1
Llava 1.5 (13B) + (a+s) (Cao et al., 2024)	X	<b>39.3</b>	<b>30.0</b>	9.8	11.4	17.7
Cambrian (8B)* + (a+s) (Cao et al., 2024)	X	<b>52.0</b>	<b>52.0</b>	14.3	15.1	23.4
PixFoundation (Llava (7B)) (Ours)	X	<b>28.7</b>	<b>28.0</b>	16.9	18.8	<b>22.7</b>
PixFoundation (Llava (13B)) (Ours)	X	<b>39.3</b>	<b>30.0</b>	<b>14.4</b>	<b>18.2</b>	<b>24.9</b>
PixFoundation (Cambrian (8B)*)) (Ours)	X	<b>52.0</b>	<b>52.0</b>	<b>17.2</b>	<b>18.9</b>	<b>27.7</b>
<b>Upper Bound - Oracle Selection</b>						
PixFoundation† (Llava (7B)) (Ours)	X	28.7	28.0	<b>26.1</b>	<b>38.0</b>	<b>32.7</b>
PixFoundation† (Llava (13B)) (Ours)	X	39.3	30.0	<b>23.6</b>	<b>38.2</b>	<b>38.7</b>
PixFoundation† (Cambrian (8B)*)) (Ours)	X	52.0	52.0	<b>52.0</b>	<b>56.1</b>	<b>54.0</b>

**Table 1.** PixMMVP benchmark evaluation of pixel-level MLLMs and baselines. We evaluate the VQA accuracy in the first and third probing (i.e.,  $\mathcal{A}^\dagger$  and  $\mathcal{A}$  resp.). Additionally, we evaluate pixel-level visual grounding with output segmentation in the first two probing (i.e.,  $\mathcal{M}^\dagger$  and  $\mathcal{M}$  resp.). \*: models using Llama 3 (8B) unlike the rest that are relying on Vicuna (7B and 13B) for the base LLM. - : indicates either the model can not be evaluated in that setting, or has low results below 1% showing complete failure in that setting.  $\mathcal{S}$ : denotes the score of the MLLM that is the harmonic mean of  $\max(\mathcal{A}, \mathcal{A}^\dagger)$  and  $\max(\mathcal{M}, \mathcal{M}^\dagger)$ . PixGr. Train: pixel-level grounding training. The oracle results are highlighted in red, and the best in each variant (7B, 13B, and 8B) are bolded.

ally, we evaluate their ability to visually ground the objects of interest in these questions.

**PixMMVP Benchmark.** Table 1 shows the results on the challenging PixMMVP benchmark. From the accuracy of VQA, MLLMs that are not trained with pixel-level grounding surpass their pixel-level counterpart with up to 16%. The best in pixel-level MLLMs score in this aspect is GLAMM-RegCap (Zhang et al., 2024b) yet it has degraded ability to generate segmentation. On the other hand, when looking at pixel-level visual grounding we find the best model, GLAMM (Rasheed et al., 2024), has a weak ability in VQA or following instructions. Moreover, it shows LISA and Llava-G are incapable of following the instruction to output the option letter reported in,  $\mathcal{A}$ . Looking at the bottom three rows, the *oracle* confirms that MLLMs that were never trained with pixel-level grounding have the correct grounding within their learned attention maps, refer to Fig. 5. Additional qualitative analysis is in Appendix B. Looking at the final score,  $\mathcal{S}$ , the oracle variant, PixFoundation† (7B), outperforms the corresponding best pixel-level MLLMs, OMG-Llava (7B), by a considerable margin while the automatic outperforms it with up to 4%. While the attend and segment baseline (Cao et al., 2024) lags behind our automatic method with more than 6%.

**PixCV-Bench Benchmark.** Table 2 shows the results on PixCV-Bench. Persistently all the pixel-level MLLMs still

lag behind the MLLMs that were never trained with pixel grounding supervision in VQA. Nonetheless, OMG-Llava strikes the right balance in both VQA and pixel-level grounding with the highest score,  $\mathcal{S}$ , within the 7B models. While, GLAMM, shows the best pixel-level grounding yet it is incapable of VQA on this benchmark. Looking at the bottom three rows for the oracle similar findings to PixMMVP emerge. The attend and segment baseline and the automatic PixFoundation baseline, both lag behind the oracle as expected yet they show competitive performance in pixel-level visual grounding, even better than some of the MLLMs trained with pixel-level supervision. Our automatic PixFoundation outperforms the attend and segment using the Llava variants, and is competitive in Cambrian-1. Cambrian-1 is more challenging as it generates more tokens, thus selecting among higher number of masks, refer to Appendix C.

**Summary.** In summary, pixel-level grounding supervision degrades MLLMs ability in VQA and sometimes even their generalization in grounding. Failure case analysis is provided in Appendix D. We show that MLLMs trained with pixel-level supervision lag behind vanilla MLLMs using simple mechanisms to extract grounding, and the *oracle* indicates there is an opportunity to improve this. Moreover, we show that grounding might not coincide with the noun phrase most similar to the referred expression, where our *oracle* upper bound is surpassing the attend and segment.

Method	PixGr. Train	CV-Bench & PixCV-Bench					$\mathcal{S}$
		$\mathcal{A}^\dagger$	$\mathcal{A}$	$\mathcal{M}$	$\mathcal{M}^\dagger$		
Llava 1.5 (7B) (Liu et al., 2023/)	✗	16.7/14.7/15.7	<b>54.2/66.5/60.4</b>	-	-	-	-
Llava 1.5 (13B) (Liu et al., 2023/)	✗	<b>14.6/16.7/15.6</b>	<b>55.6/67.1/61.3</b>	-	-	-	-
Cambrian (8B)* (Tong et al., 2024a)	✗	<b>55.7/68.7/62.2</b>	<b>65.2/79.1/72.2</b>	-	-	-	-
OMG Llava (7B) (Zhang et al., 2024b)	✓	9.2/14.7/12.0	36.8/47.4/42.1	-	50.5	<b>45.9</b>	-
GLAMM (7B) (Rasheed et al., 2024)	✓	-	-	<b>30.2</b>	<b>51.9</b>	-	-
GLAMM - RCap (7B) (Rasheed et al., 2024)	✓	<b>22.8/32.8/27.8</b>	46.8/62.0/54.4	3.6	7.4	13.0	-
LISA (7B) (Lai et al., 2024)	✓	1.9/5.5/3.7	-	16.8	48.1	6.7	-
Llava-G (7B) (Zhang et al., 2024a)	✓	13.9/14.2/14.1	5.1/3.7/4.4	1.7	17.6	15.8	-
Llava 1.5 (7B) + (a+s) (Cao et al., 2024)	✗	16.7/14.7/15.7	<b>54.2/66.5/60.4</b>	5.2	15.6	24.8	-
Llava 1.5 (13B) + (a+s) (Cao et al., 2024)	✗	<b>14.6/16.7/15.6</b>	<b>55.6/67.1/61.3</b>	<b>4.7</b>	14.9	24.0	-
Cambrian (8B)* + (a+s) (Cao et al., 2024)	✗	<b>55.7/68.7/62.2</b>	<b>65.2/79.1/72.2</b>	<b>18.6</b>	15.9	<b>29.6</b>	-
PixFoundation (Llava (7B)) (Ours)	✗	16.7/14.7/15.7	<b>54.2/66.5/60.4</b>	<b>5.3</b>	<b>19.1</b>	29.0	-
PixFoundation (Llava (13B)) (Ours)	✗	<b>14.6/16.7/15.6</b>	<b>55.6/67.1/61.3</b>	<b>4.7</b>	<b>17.7</b>	<b>27.5</b>	-
PixFoundation (Cambrian (8B)*)(Ours)	✗	<b>55.7/68.7/62.2</b>	<b>65.2/79.1/72.2</b>	12.1	<b>16.6</b>	27.0	-
<b>Upper Bound - Oracle Selection</b>							
PixFoundation† (Llava (7B)) (Ours)	✗	16.7/14.7/15.7	54.2/66.5/60.4	<b>6.3</b>	<b>49.7</b>	<b>54.5</b>	-
PixFoundation† (Llava (13B)) (Ours)	✗	14.6/16.7/15.6	55.6/67.1/61.3	<b>5.3</b>	<b>50.6</b>	<b>55.4</b>	-
PixFoundation† (Cambrian (8B)*)(Ours)	✗	55.7/68.7/62.2	65.2/79.1/72.2	<b>54.3</b>	<b>64.4</b>	<b>68.1</b>	-

Table 2. **PixCV-Bench** benchmark evaluation of the various pixel-level MLLMs and the different baselines. We evaluate VQA accuracy in the first and third probing (i.e.,  $\mathcal{A}$ ,  $\mathcal{A}^\dagger$  resp.). Note, we show the accuracies as ././. for the ADE20K, COCO and the average of both respectively. Additionally, we evaluate pixel-level visual grounding ability with output segmentation masks in the first two probing (i.e.,  $\mathcal{M}^\dagger$ ,  $\mathcal{M}$  resp.). \*: models using Llama 3 (8B) unlike the rest that are relying on Vicuna (7B and 13B) for the base LLM. GLAMM-RCap: is the GLAMM-RegCap variant. - : indicates either the model can not be evaluated in that setting, or has low results below 1% showing complete failure in that setting.  $\mathcal{S}$ : denotes the score of the MLLM that is the harmonic mean of  $\max(\mathcal{A}, \mathcal{A}^\dagger)$  and  $\max(\mathcal{M}, \mathcal{M}^\dagger)$ . PixGr. Train: pixel-level grounding training. The oracle results are highlighted in red, and the best in each variant (7B, 13B, and 8B) are bolded.

### 4.3. When does grounding emerge in MLLMs?

**When - location.** Taking into account the powerful performance of the *oracle* upper bound, it begs the important question of when grounding emerges. We start by looking at when it emerges in terms of the location within the output text. We analyze the word/phrase location with respect to the full output text in terms of a percentage from its total length, (i.e., 0% means the beginning of the text). Accordingly, Fig. 6a shows the location percentages histogram, binned at 10%, for the three base MLLMs reporting the oracle selection and evaluating on PixMMVP benchmark using the second probing. In the Llava 1.5 variants, grounding mostly emerges at the last 40% of the output text, while for Cambrian it is mostly at the last 10%.

**When - concept.** For the second analysis we look into the concept category that the correct output word/phrase corresponds to. The previous assumption in other works is that grounding emerges in exact noun or noun phrase of the object of interest. Except our analysis confirms that this is not necessarily the case. We take the correct noun/noun phrase where the grounding emerges based on the *oracle* from all the three variants, then we pass it to GPT-4o to request a grouping of these concepts. Specifically, we prompt it with the following “*Can you group these noun phrases into categories of abstract concepts. You are provided with pairs*

*of (noun phrase, its full context).*”, where the entire output text is the full context. After manual filtration and merging it resulted into six main groups, which are: (i) Color and appearance, (ii) location and position, (iii) object parts, (iv) context and setting, (v) objects and entities, and (vi) State. We then prompt for each of the noun/noun phrase, GPT-4o, to categorize it within these six categories. The histogram of the occurrences of these concept categories is shown in Fig. 6b. It clearly conveys that in certain scenarios the correct output when grounding emerges can be describing the position or the location of the object of interest not necessarily the exact ground-truth referring expression. While the majority occurs under “Objects and Entities”, there are still percentage of output coinciding with position, color, context, object part, or even the state. Further qualitative results are provided in the Appendix B.

**Random vs. best.** All the results of our baselines and our findings hinge on the fact that we are using the maximum attention per output noun phrase to prompt SAM for the segmentation mask. Nonetheless, as a lower bound analysis, we evaluate the performance if we use a random point as prompt to SAM instead. For fair comparison, we generate random points with the count of output masks that the oracle has to select among (i.e., the number of the output noun phrases). We conduct this ablation on PixMMVP using

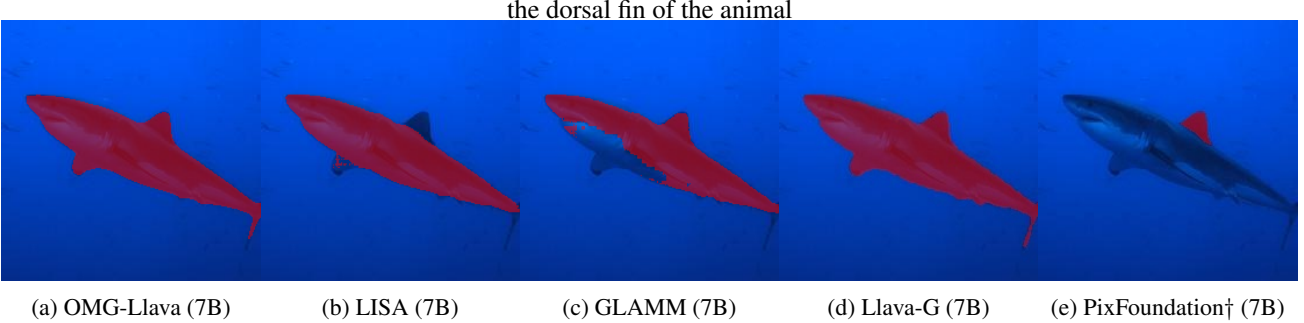


**Figure 5.** PixMMVP qualitative comparison in pixel-level visual grounding following the second probing technique. The referred expression is shown on top. It shows that mining for the grounding within the attention maps of vanilla MLLMs using their upper bound is better than MLLMs trained with pixel-level supervision, without degrading their VQA abilities. Thus, questioning whether the current training paradigm of pixel-level MLLMs is in the right direction.

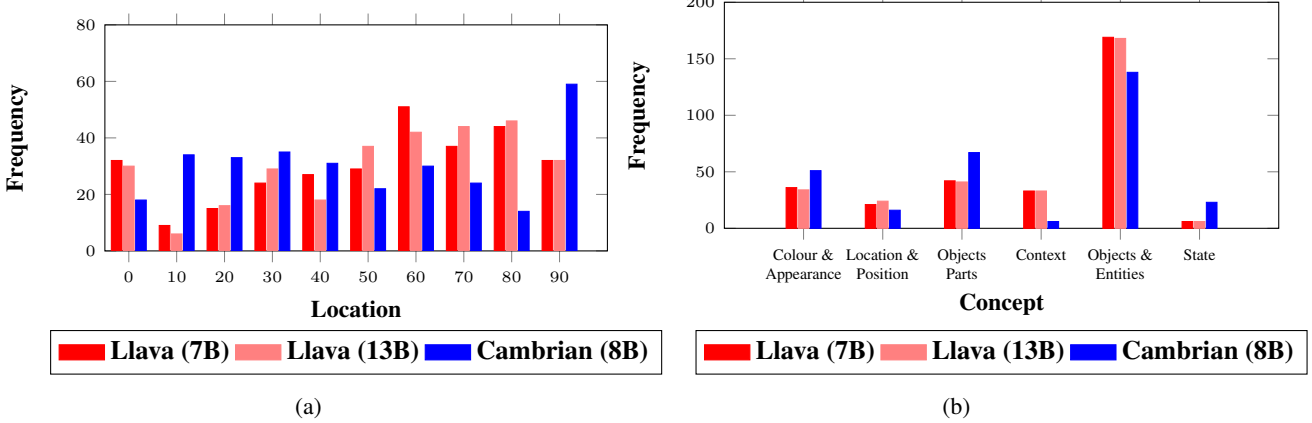


**Figure 6.** Analysis on when grounding emerges on PixMMVP benchmark using the three base MLLMs, Llava 1.5 (7, 13B) and Cambrian-1 (8B), that were not trained with pixel-level grounding supervision. We follow the second probing then report the oracle selection. Analysis on: (a) the output location and (b) the output concept category, that coincides with the best segmentation.

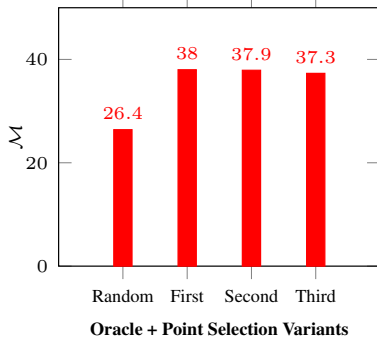


**Figure 7.** Ablation on the point prompt used paired with the *oracle* selection on PixMMVP. We evaluate using the second probing reporting mean intersection over union,  $\mathcal{M}$ .

Llava 1.5 (7B) base MLLM, with random point prompts followed by the *oracle* selection among their SAM masks. Figure 7 shows that this random + oracle baseline is a strong baseline, yet it lags behind the correct one using the maximum point (i.e., First) with around 12%. More importantly, we confirm the stability of the results if we select the second best or third best attention (i.e., Second and Third), which

are on-par to the maximum point. Thus, even with the oracle selection, using the wrong point prompts lags with a considerable margin behind using the correct ones.

**Summary.** In summary, we found that grounding emerges in the last 40% of the output text which might indicate that the reasoning of the model to provide a response impacts when the correct visual grounding can occur. More importantly, we show that grounding in MLLMs can emerge in the noun phrase that corresponds to color, position or other characteristics of the object of interest and not necessarily the exact referring expression.

## 5. Conclusion

We proposed two benchmarks showing that pixel-level MLLMs degraded the ability in VQA and even grounding of fine-grained objects. Thus, our results questioned whether we are heading in the right direction with these models. Additionally, we provide powerful baselines with improved scores without training for pixel-level grounding.

## Impact Statement

Multi-modal large language models are widely used in various applications, such as robotics, medical image processing and remote sensing. The pixel-level understanding within such MLLMs is necessary for such applications that require the localization and even in certain scenarios the delineation of the boundaries for the objects of interest. It is even more important to maintain a good chat performance and visual question answering ability in such applications as well. In our work, we have investigated the shortcomings of pixel-level MLLMs while providing more challenging benchmarks for these, to improve them further.

However, as with many other AI advancements there are risks that could be entailed from the deployment of such models. There could be inherent biases emerging in such pixel-level MLLMs impacting various under-represented groups. We think that our benchmarking efforts and providing a tool to understand the pitfalls in the understanding and reasoning of these models could be an initial direction for mitigating such biases. Nonetheless, we leave it for future work to explore this further.

## References

- Bommasani, R., Hudson, D. A., Adeli, E., Altman, R., Arora, S., von Arx, S., Bernstein, M. S., Bohg, J., Bosse-lut, A., Brunskill, E., et al. On the opportunities and risks of foundation models. *arXiv preprint arXiv:2108.07258*, 2021.
- Cao, S., Gui, L.-Y., and Wang, Y.-X. Emerging pixel grounding in large multimodal models without grounding supervision. *arXiv preprint arXiv:2410.08209*, 2024.
- Dai, W., Li, J., Li, D., Tiong, A., Zhao, J., Wang, W., Li, B., Fung, P., and Hoi, S. InstructBLIP: Towards general-purpose vision-language models with instruction tuning. In *Advances in Neural Information Processing Systems*, 2023. URL <https://openreview.net/forum?id=vvoWPYqZJA>.
- Dutta, A., Gupta, A., and Zissermann, A. VGG image annotator (VIA). <http://www.robots.ox.ac.uk/vgg/software/via/>, 2016.
- Hajimiri, S., Ayed, I. B., and Dolz, J. Pay attention to your neighbours: Training-free open-vocabulary semantic segmentation. *Proceedings of the Conference on Winter Applications and Computer Vision*, 2025.
- Honnibal, M., Montani, I., Van Landeghem, S., and Boyd, A. spacy: Industrial-strength natural language processing in python. <https://spacy.io/>, 2020.
- Kazemzadeh, S., Ordóñez, V., Matten, M., and Berg, T. Referitgame: Referring to objects in photographs of natural scenes. In *Proceedings of the Conference on Empirical Methods in Natural Language Processing (EMNLP)*, pp. 787–798, 2014.
- Kirillov, A., Mintun, E., Ravi, N., Mao, H., Rolland, C., Gustafson, L., Xiao, T., Whitehead, S., Berg, A. C., Lo, W.-Y., et al. Segment anything. In *Proceedings of the IEEE/CVF International Conference on Computer Vision*, pp. 4015–4026, 2023.
- Lai, X., Tian, Z., Chen, Y., Li, Y., Yuan, Y., Liu, S., and Jia, J. Lisa: Reasoning segmentation via large language model. In *Proceedings of the IEEE/CVF Conference on Computer Vision and Pattern Recognition*, pp. 9579–9589, 2024.
- Lin, T.-Y., Maire, M., Belongie, S., Hays, J., Perona, P., Ramanan, D., Dollár, P., and Zitnick, C. L. Microsoft coco: Common objects in context. In *Proceedings of the European Conference on Computer Vision, Part V 13*, pp. 740–755. Springer, 2014.
- Liu, H., Li, C., Wu, Q., and Lee, Y. J. Visual instruction tuning. *Advances in Neural Information Processing Systems*, 36, 2023/.
- Liu, H., Li, C., Li, Y., and Lee, Y. J. Improved baselines with visual instruction tuning. In *Proceedings of the IEEE/CVF Conference on Computer Vision and Pattern Recognition*, pp. 26296–26306, 2024.
- Luo, J., Khandelwal, S., Sigal, L., and Li, B. Emergent open-vocabulary semantic segmentation from off-the-shelf vision-language models. In *Proceedings of the IEEE Conference on Computer Vision and Pattern Recognition*, pp. 4029–4040, 2024.
- Minaee, S., Boykov, Y., Porikli, F., Plaza, A., Kehtarnavaz, N., and Terzopoulos, D. Image segmentation using deep learning: A survey. *IEEE Transactions on Pattern Analysis and Machine Intelligence*, 44(7):3523–3542, 2021.
- Radford, A., Kim, J. W., Hallacy, C., Ramesh, A., Goh, G., Agarwal, S., Sastry, G., Askell, A., Mishkin, P., Clark, J., et al. Learning transferable visual models from natural language supervision. In *Proceedings of the International Conference on Machine Learning*, pp. 8748–8763. PMLR, 2021.
- Rasheed, H., Maaz, M., Shaji, S., Shaker, A., Khan, S., Cholakkal, H., Anwer, R. M., Xing, E., Yang, M.-H., and Khan, F. S. Glamm: Pixel grounding large multimodal model. In *Proceedings of the IEEE/CVF Conference on Computer Vision and Pattern Recognition*, pp. 13009–13018, 2024.

- Ravi, N., Gabeur, V., Hu, Y.-T., Hu, R., Ryali, C., Ma, T., Khedr, H., Rädle, R., Rolland, C., Gustafson, L., et al. Sam 2: Segment anything in images and videos. *arXiv preprint arXiv:2408.00714*, 2024.
- Tong, S., II, E. L. B., Wu, P., Woo, S., IYER, A. J., Akula, S. C., Yang, S., Yang, J., Middepogu, M., Wang, Z., Pan, X., Fergus, R., LeCun, Y., and Xie, S. Cambrian-1: A fully open, vision-centric exploration of multimodal LLMs. In *Advances in Neural Information Processing Systems*, 2024a. URL <https://openreview.net/forum?id=Vi8AepAXGy>.
- Tong, S., Liu, Z., Zhai, Y., Ma, Y., LeCun, Y., and Xie, S. Eyes wide shut? exploring the visual shortcomings of multimodal llms. In *Proceedings of the IEEE/CVF Conference on Computer Vision and Pattern Recognition*, pp. 9568–9578, 2024b.
- Wang, F., Mei, J., and Yuille, A. Sclip: Rethinking self-attention for dense vision-language inference. In *Proceedings of the European Conference on Computer Vision*, pp. 315–332. Springer, 2024.
- Wang, Q., Chang, Y.-Y., Cai, R., Li, Z., Hariharan, B., Holynski, A., and Snavely, N. Tracking everything everywhere all at once. In *Proceedings of the IEEE/CVF International Conference on Computer Vision*, pp. 19795–19806, 2023.
- Wolf, T., Debut, L., Sanh, V., Chaumond, J., Delangue, C., Moi, A., Cistac, P., Rault, T., Louf, R., Funtowicz, M., et al. Huggingface’s transformers: State-of-the-art natural language processing. arxiv. *arXiv preprint arXiv:1910.03771*, 2019.
- Yang, L., Kang, B., Huang, Z., Xu, X., Feng, J., and Zhao, H. Depth anything: Unleashing the power of large-scale unlabeled data. In *Proceedings of the IEEE/CVF Conference on Computer Vision and Pattern Recognition*, pp. 10371–10381, 2024.
- Yu, L., Poirson, P., Yang, S., Berg, A. C., and Berg, T. L. Modeling context in referring expressions. In *Proceedings of the European Conference on Computer Vision, Amsterdam, The Netherlands, Part II 14*, pp. 69–85. Springer, 2016.
- Yue, X., Ni, Y., Zhang, K., Zheng, T., Liu, R., Zhang, G., Stevens, S., Jiang, D., Ren, W., Sun, Y., et al. Mmmu: A massive multi-discipline multimodal understanding and reasoning benchmark for expert agi. In *Proceedings of the IEEE/CVF Conference on Computer Vision and Pattern Recognition*, pp. 9556–9567, 2024.
- Zhang, H., Li, H., Li, F., Ren, T., Zou, X., Liu, S., Huang, S., Gao, J., Li, C., Yang, J., et al. Llava-grounding: Grounded visual chat with large multimodal models. In *Proceedings of the European Conference on Computer Vision*, pp. 19–35. Springer, 2024a.
- Zhang, T., Li, X., Fei, H., Yuan, H., Wu, S., Ji, S., Loy, C. C., and Yan, S. Omg-llava: Bridging image-level, object-level, pixel-level reasoning and understanding. *arXiv preprint arXiv:2406.19389*, 2024b.
- Zhou, B., Zhao, H., Puig, X., Fidler, S., Barriuso, A., and Torralba, A. Scene parsing through ade20k dataset. In *Proceedings of the IEEE Conference on Computer Vision and Pattern Recognition*, pp. 633–641, 2017.
- Zhou, T., Porikli, F., Crandall, D. J., Van Gool, L., and Wang, W. A survey on deep learning technique for video segmentation. *IEEE Transactions on Pattern Analysis and Machine Intelligence*, 45(6):7099–7122, 2022.

## A. Additional implementation details

In this section, we cover additional details about our proposed datasets and the implementation of the evaluation setup and baselines. We also refer to the output from the questions of the three probing techniques in the supplementary material for all the studied models.

**Datasets.** Our proposed datasets, PixMMVP and PixCV-Bench, are composed of ground-truth referring expressions describing the object of interest in the respective question and its segmentation mask. We show in Fig. 8 examples of these ground-truth annotations for both datasets. It shows the challenging scenarios in pixel-level visual grounding which is strongly tied to the visual question answering task, since an integral part of answering these questions requires the grounding of the object/s of interest.

**Models.** We also detail the model checkpoints we use for the four pixel-level MLLMs and their variants, retrieved from HuggingFace (Wolf et al., 2019) in Table 3. These also include the model checkpoints used for the base MLLMs that were not trained with pixel-level visual grounding. It is worth noting, that for GLAMM we use two variants (FullScope and RegCap) since their base model (i.e., FullScope) has low performance in the visual question answering task. As such we use the other variant for GLAMM that was fine-tuned for region-level captioning using RefCOCOg and Visual Genome dataset. Furthermore, we provide details on the *oracle* selection mechanism, where in the case of multiple masks exhibiting the same IoU we select the last occurring one in the when analysis, since we need to select the location of when it occurs. While in the quantitative and qualitative evaluation, we resort to simply not selecting any mask. These occur in few cases when the ground-truth mask is all background, thus any mask IoU will result in zero.

Additionally, we provide details on the SAM model that is used in the three baselines and upper bounds in our benchmarks, where we use the ViT-H variant. Finally, we provide an illustrative example of our automatic selection mechanism with the corresponding predictions on PixMMVP using Llava 1.5 (7B) in Fig. 9. Our automatic selection goes through an iterative process of prompting the selected MLLM, in our case Cambrian-1, with three images overlaid with predicted segmentation to select the best within each group of three. In the final stage the best images are used to prompt the MLLM to select the final selected mask that best describes the object of interest. In the *oracle* upper bound whenever the model is to be evaluated in a multiple object scenario we take all the possible pairs of the masks then select the best pair based on the highest intersection over union.

**Evaluation.** We also provide the details on computing the

Model Name	Model Checkpoint
LISA	xinlai/LISA-7B-v1-explanatory
GLAMM	MBZUAI/GLaMM-FullScope
GLAMM-RegCap	MBZUAI/GLaMM-RegCap-RefCOCOg
Llava-G	Haozhangcx/llava_grounding_gd_vp
Llava 1.5 (7B)	4bit/llava-v1.5-7b
Llava 1.5 (13B)	4bit/llava-v1.5-13b-3GB
Cambrian-1 (8B)	nyu-visionx/cambrian-8b

Table 3. Hugging Face model checkpoints used in our benchmarks.

visual question answering accuracy using GPT-4o in the first protocol (Tong et al., 2024b). We use the following prompt: “Given the following question <QUESTION>, the correct answer is <ANSWER>. Does the following answer correctly answers the question, answer: <RESPONSE>? Respond with a Yes/No”.

## B. Additional qualitative analysis

In this section, we provide a qualitative ablation of our baselines and a visualization of the attention maps that can show how vanilla MLLMs are reasoning on the question they are answering. Additionally, we provide qualitative examples showing when grounding emerges in these vanilla MLLMs. Finally, we provide more examples on PixMMVP and PixCV-Bench benchmarks.

### B.1. Baselines ablation

We show the qualitative ablation among the two baselines and upper bound using the best base MLLM Cambrian-1 (8B) in Fig. 10 on PixMMVP. The three confirm that there is grounding emerging in MLLMs that were not trained with pixel-level grounding supervision. Nonetheless, it shows that identifying when that grounding emerges is equally important in retrieving the best segmentation of the referring expression. The first baseline, attend and segment, assumes the alignment between the attention map that can be mined for the segmentation mask and the noun phrase that has the highest correspondence to the ground-truth category or noun phrase. Our findings quantitatively and qualitatively show otherwise, where grounding can emerge in different output tokens. It also shows the *oracle* upper bound for mask selection, PixFoundation†, exhibiting better segmentation than the attend and segment, confirming on the aforementioned finding. Additionally, it shows that our simple automatic mechanism, PixFoundation, surpasses the attend and segment as well on PixMMVP.

### B.2. Attention maps visualization

In this section, we visualize the normalized attention maps,  $\tilde{A}$ , in Fig. 11. We show two examples for Cambrian-1 (8B) from PixMMVP using the first probing where we di-



Figure 8. Examples of ground-truth annotations for referring expressions in the respective object of interest in the question and their segmentation masks. First row: PixMMVP examples, Second row: PixCV-Bench examples. Ground-truth highlighted in green.

rectly prompt the model with question and options. The first row shows outstanding ability to visually ground the different noun phrases from the output text. The full output text of the first row example is: “*The image provided is a cake designed to resemble a minion from the Despicable Me franchise. It is not a living creature and therefore cannot smile or have a tongue out. The cake is an inanimate object, crafted to mimic the appearance of a minion, which is a fictional character from the animated movie series. The design elements such as the yellow skin, blue overalls, and goggles are characteristic of the minions’ appearance in the films.*” The visualization shows how the maximally attended locations for the last three noun phrases correspond to the correct locations in the image.

The second output text corresponding to the example shown is; “*The butterfly’s feet, also known as tarsi, are not distinctly visible in this image due to the angle and the butterfly’s wings being open. However, we can infer their presence and approximate location. Monarch butterflies have six legs, with the hind legs being the longest and the front legs being the shortest. The legs are typically slender and have a hairy texture, which aids in gripping onto surfaces. In this image, the legs are likely located at the bottom of the butterfly’s body, just below the abdomen, and are probably in contact with the leaf it is perched on.*” The attention maps highlight what we suspect is a failure where the MLLM mistakes the antenna of the butterfly for front legs. Such hidden failures that do not necessarily affect the correctness of the answer, are still important to study and we believe our tool with the oracle upper bound can be used to inspect this further. Finally, we find that these attention maps in both examples are not sufficiently accurate to be used for segmentation directly, yet when paired with a powerful segmentation method like

SAM it provides a good segmentation performance.

### B.3. When does grounding emerge?

We show additional examples on when grounding emerges in multi-modal large language models, specifically in the Llava 1.5 (7B) variant, using the second probing to prompt the model to segment what is in the referring expression. Figures 12, 14, 13, 15 and 16 show the corresponding predicted masks for the grounding that emerged highlighted in red with the maximum attention point as a black dot. Figure 17 shows the aforementioned five examples with the input prompt, the concept category and the noun phrase corresponding to the best grounding using the *oracle* selection and the full output text. It clearly shows that the correct output token can correspond to location or color but not necessarily the ground-truth referring expression. While some of the noun phrases and their masks from the point prompting of SAM do correspond to what the noun phrase is describing. It is not always the case, example in Fig. 14 “the flame” was not able to highlight the correct object yet it appeared in the noun phrase corresponding to the location “the top”. It also shows that the majority of correct grounding occurs near the end of the output text after the model reasoned for an answer to the question.

Additionally, this type of mining for attention maps can show potential mistakes that MLLMs fall into while performing the grounding to reason on what is in the image. An example on that is in Fig. 15, where the model potentially mistakes a crack in the wood for the minute hand. Figure 16 shows another clear example, where the MLLM thinks it is seeing a tongue highlighting its potential place near the mouth. Yet the image does not really have the tongue out

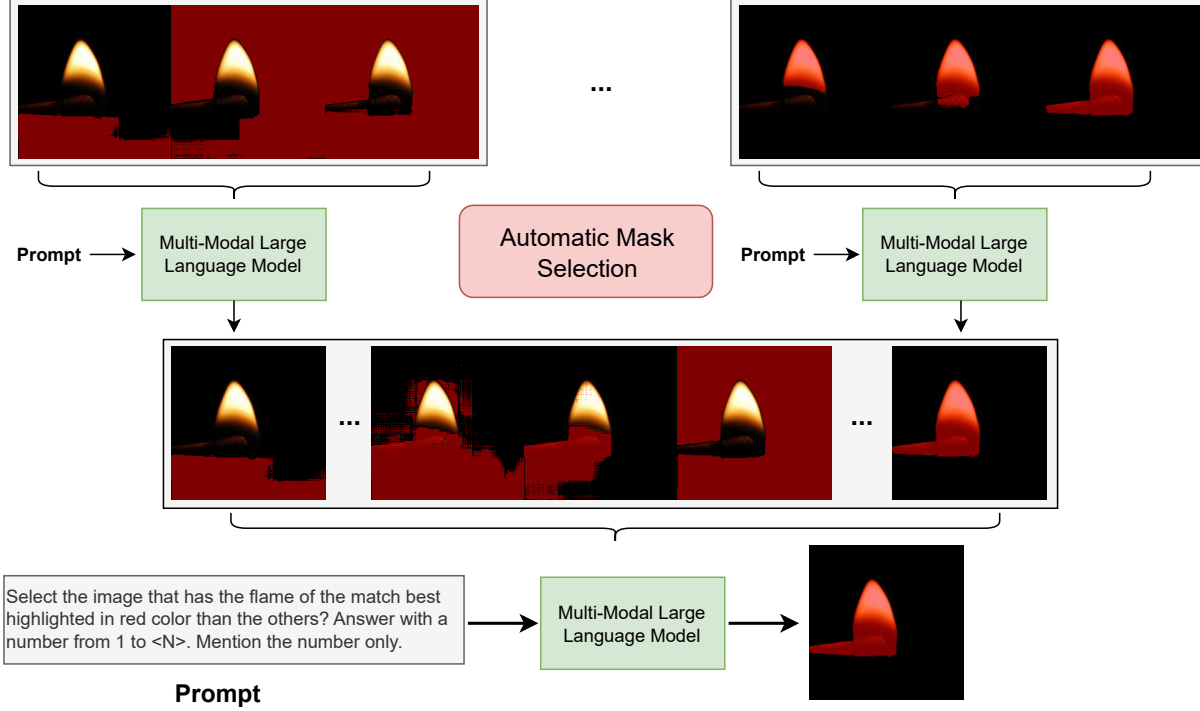


*Figure 9.* The automatic selection baseline, PixFoundation, which uses a simple mechanism of highlighting the predicted masks in red then prompting a multi-modal large language model to select the right mask from the group of highlighted images, followed by the final mask selection.

and consequently the error in the grounding lead to an error in the visual question answering. Thus, our PixFoundation $\dagger$  serves as an interesting tool to interpret and understand how MLLMs work and reason to produce the final output with the *oracle* selection as an upper bound. Yet, there is an open question on how to identify the real mistake from the MLLM vs. simple misalignment between the noun phrase and the grounding emerging, since grounding could emerge with phrases describing it or parts of it instead of the object’s noun phrase itself. We leave this for future work.

#### B.4. PixMMVP benchmark

Figure 18 shows additional results on PixMMVP benchmark comparing different pixel-level MLLMs with our *oracle* baseline using Llava 1.5 (7B). While GLAMM shows strong pixel-level visual grounding yet we have shown earlier that it is almost incapable of visual question answering which renders the model weak for general purpose tasks. On the other hand, OMG-Llava shows a better balance in pixel-level visual grounding and visual question answering as previously detailed. Nonetheless, the simple mining of attention maps from Llava 1.5 (7B) using the *oracle* selection which we call PixFoundation $\dagger$  shows the strongest capability in both grounding and VQA. In fact, certain MLLMs

that were trained with pixel-level visual grounding, such as LISA, have degraded the performance with respect to the hidden information already existing in powerful MLLMs that were not trained with such supervision.

#### B.5. PixCV-Bench benchmark

Figure 19 shows qualitative results on PixCV-Bench. It shows that pixel-level MLLMs struggle with segmenting the object annotated by the red box unlike our *oracle* baseline, PixFoundation $\dagger$ . Indeed the attention maps from these MLLMs are looking at the right object annotated by the red box without receiving any pixel-level grounding supervision during training.

### C. Analysis on the output length

In this section, we provide additional analysis on the output length on average through PixMMVP dataset using the first and second probing schemes. Specifically, we report the output length as the number of characters in the output, and the number of noun phrases extracted from it. The reason to study this, since it has relation to the number of noun phrases and consequently the number of masks our baselines are selecting among. Table 4 shows the average output

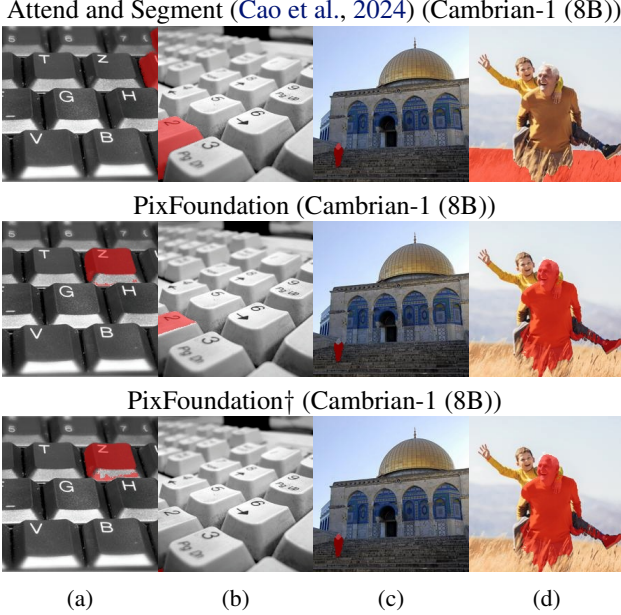


Figure 10. Baselines and upper bound ablation using the base MLLM, Cambrian-1 (8B), ablating the different schemes for mask selection. We use the second probing to prompt the MLLM to identify the referred expression. The referring expressions for these examples are as follows: (a) the key “z”, (b) the key “z”, (c) people, (d) the elderly person. Predictions are highlighted in red.

Model Name	Probing	Output Length	# Noun Phrases
Llava 1.5 (7B)	First	44.2	2.3
Llava 1.5 (13B)	First	45.3	2.4
Cambrian-1 (8B)	First	313.8	15.2
Llava 1.5 (7B)	Second	92.6	5.2
Llava 1.5 (13B)	Second	97.2	5.5
Cambrian-1 (8B)	Second	561.3	27.3

Table 4. The average output length across PixMMVP dataset for the three base MLLMs using the first and second probing techniques.

length computed across PixMMVP dataset, comparing the three base MLLMs. We notice that Cambrian-1 (8B) generates longer outputs with a considerable margin than Llava variants. Hence, we believe the superiority of the *oracle* upper bound with Cambrian-1 in the grounding has strong correlation to producing longer outputs with more attention maps to mine and select from, than Llava variants. Nonetheless, it makes it more challenging for the automatic baseline which explains its results on PixCV-Bench with respect to the attend and segment. We believe the use of GPT-4o for the automatic selection instead of Cambrian-1 (8B) should improve these results further.

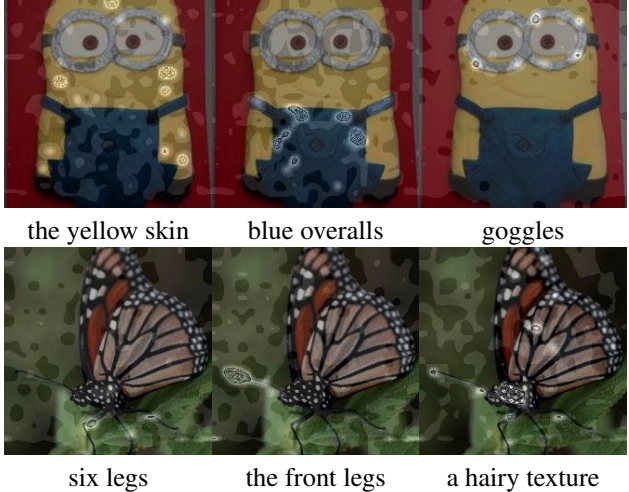


Figure 11. Normalized attention maps visualization showing the noun phrase and its corresponding attention in the output text for two PixMMVP examples using Cambrian-1 (8B) base MLLM. While the attention maps can not be directly used as segmentation, yet it provides initial locations for the maximally attended pixels corresponding to what the model is looking at. In certain scenarios it exactly aligns with the noun phrase describing it as in the two examples. Yet in certain scenarios as we showed earlier, the grounding of the referred expression in question emerges with other noun phrases describing it.

## D. Failure Cases Analysis

In this section, we conduct additional failure case analysis of pixel-level MLLMs and our baselines qualitatively and quantitatively.

### D.1. Failures in Visual Question Answering

We start with a fine-grained quantitative analysis of how the studied models perform across PixMMVP and PixCV-Bench. For PixMMVP we follow their scheme to identify the nine visual patterns and report the model’s accuracy with each pattern in Fig. 20. Similarly, we show fine-grained analysis relying on the tasks for the two datasets (ADE20K and COCO) in Fig. 21.

PixMMVP results show that the majority of pixel-level MLLMs, highlighted in blue, suffer in the state, orientation and quantity related tasks. On the other hand, relational context, color and presence of features show the best performance with pixel-level MLLMs. Nonetheless, across all the visual patterns, the MLLMs that were not trained with pixel-level supervision persistently surpass these pixel-level MLLMs with a considerable margin. PixCV-Bench, similarly shows the count task is more challenging than the relational positioning. It also shows that ADE20K dataset serves as a more challenging dataset than COCO.

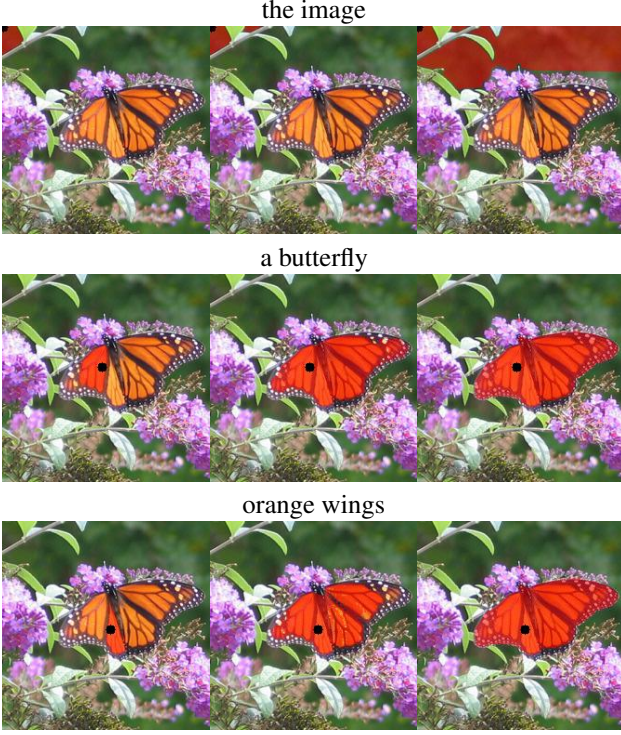


*Figure 12.* First example of when grounding emerges, corresponding to Image 1 in Fig. 17. Each row has the corresponding noun phrase on top and three potential SAM predicted masks highlighted in red using the maximum attention point of this noun phrase as a point prompt, highlighted as a black dot. It shows the output from mining the attention maps for pixel-level grounding using Llava 1.5 (7B) base MLLM.

## D.2. Failures in Pixel-level Visual Grounding

Finally, we show qualitatively the failure cases of the *oracle* upper bound in Fig. 22. It shows failures in segmenting all the object instances in the first row, since the current point prompting assumes one connected component corresponding to each expression. However, certain scenarios, such as the image with the spots on the animal, can lead to these failures in the oracle even when the localisation of some of these is correct. Mechanisms that solve this multi instance scenarios of the same object are left for future work.

Another failure occurring such as in the second row stems from ambiguity in the referring expression itself or failures from SAM identifying the separation between the wall and the ceiling. Hence, the oracle upper bound is generally inheriting SAM failures. However, its main purpose of showing that the hidden information within powerful MLLMs is sufficient to perform pixel-level grounding is achieved, and even surpassing pixel-level MLLMs without degrading their VQA abilities.

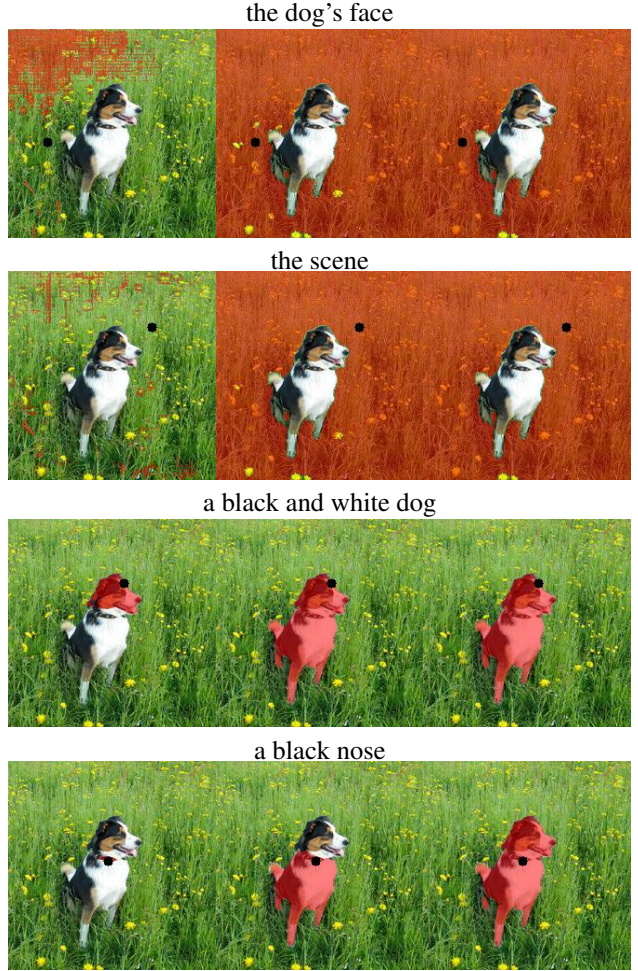


*Figure 13.* Third example of when grounding emerges, corresponding to Image 6 in Fig. 17. Each row has the corresponding noun phrase on top and three potential SAM predicted masks highlighted in red using the maximum attention point of this noun phrase as a point prompt, highlighted as a black dot. It shows the output from mining the attention maps for pixel-level grounding using Llava 1.5 (7B) base MLLM.

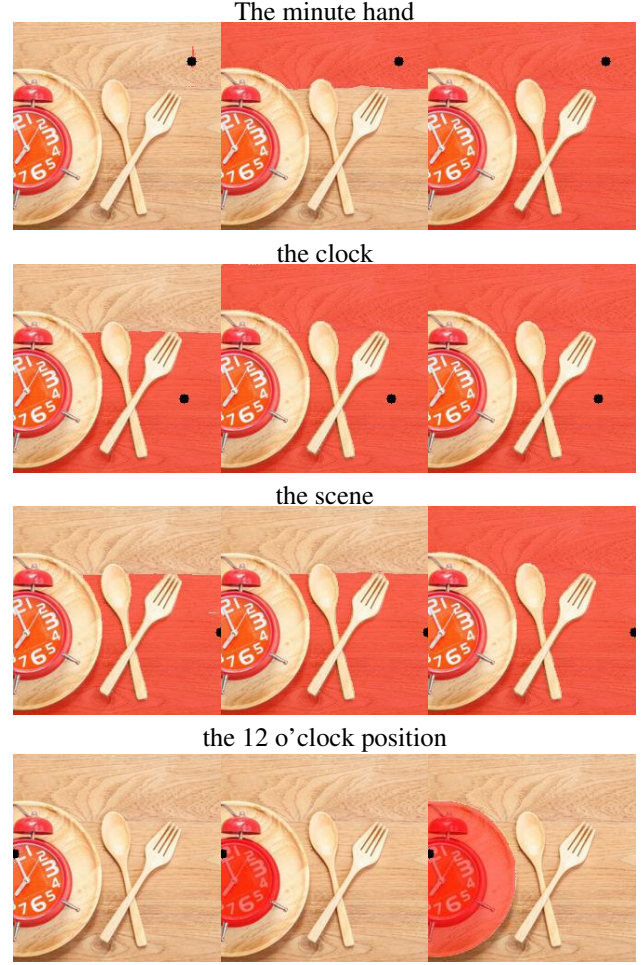
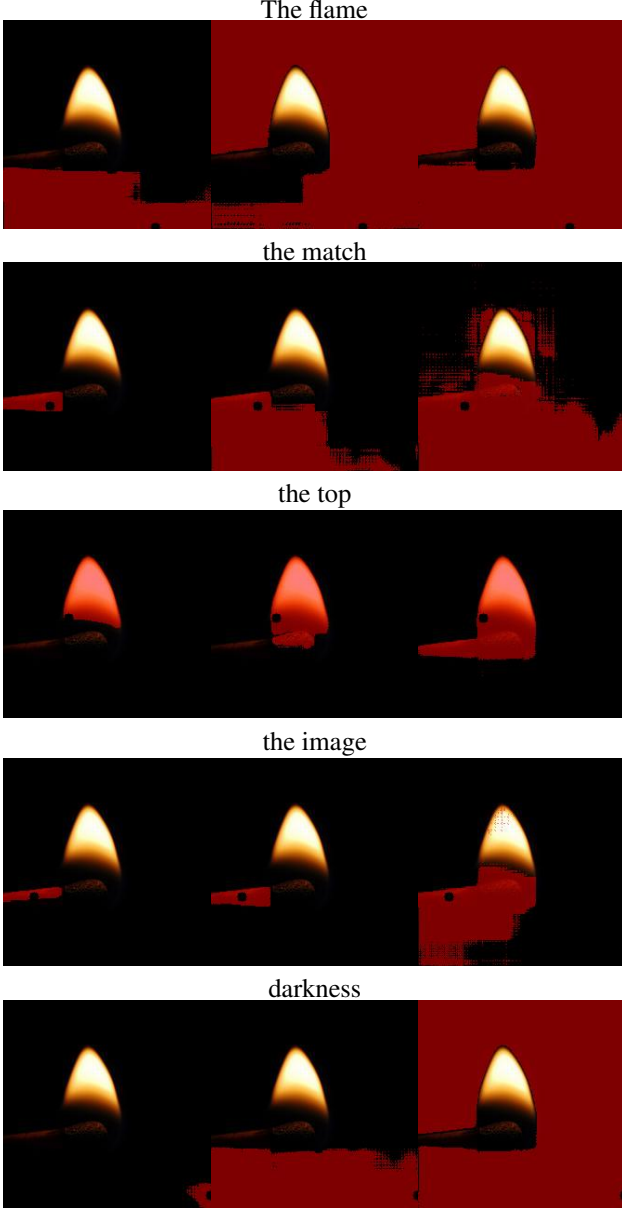


*Figure 14.* Second example of when grounding emerges, corresponding to Image 3 in Fig. 17. Each row has the corresponding noun phrase on top and three potential SAM predicted masks highlighted in red using the maximum attention point of this noun phrase as a point prompt, highlighted as a black dot. It shows the output from mining the attention maps for pixel-level grounding using Llava 1.5 (7B) base MLLM.

*Figure 15.* Fourth example of when grounding emerges, corresponding to Image 161 in Fig. 17. Each row has the corresponding noun phrase on top and three potential SAM predicted masks highlighted in red using the maximum attention point of this noun phrase as a point prompt, highlighted as a black dot. It shows the output from mining the attention maps for pixel-level grounding using Llava 1.5 (7B) base MLLM.

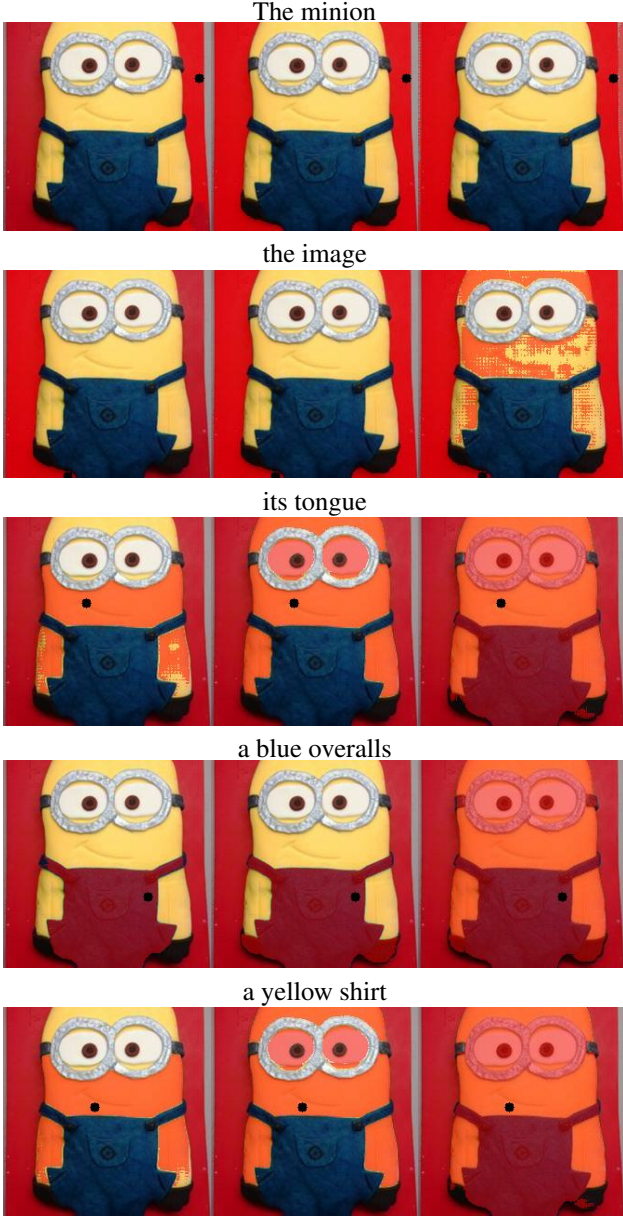


*Figure 16.* Fifth example of when grounding emerges, corresponding to Image 292 in Fig. 17. Although the ground-truth segmentation is all background, since the *oracle* selection sees all the candidate masks with IoU zero, it defaults to the last selection. Each row has the corresponding noun phrase on top and three potential SAM predicted masks highlighted in red using the maximum attention point of this noun phrase as a point prompt, highlighted as a black dot. It shows the output from mining the attention maps for pixel-level grounding using Llava 1.5 (7B) base MLLM.

Image	Prompt	Concept Category	Noun Phrase	Output
1	Identify the butterfly's wings in the scene.	Color & Appearance	orange wings	In the image, there is a butterfly with orange wings.
3	Identify the flame of the match in the scene.	Location & Position	the top	The flame of the match is located at the top of the image, surrounded by darkness.
6	Identify the dog's face in the scene.	Color & Appearance	a black and white dog	The dog's face in the scene is a black and white dog with a black nose.
161	Identify the minute hand of the clock in the scene.	Location & Position	the 12 o'clock position	The minute hand of the clock in the scene is located at the 12 o'clock position.
292	Identify the minion in the image smiling with its tongue out in the scene.	Color & Appearance	a yellow shirt	The minion in the image is smiling with its tongue out, wearing a blue overalls and a yellow shirt.


1

3

6

161

292

Figure 17. Examples of the noun phrases and concept categories where the grounding emerged corresponding to the provided referring expression as input to the MLLM following the third evaluation protocol. The base MLLM used in these experiments are Llava 1.5 7B.

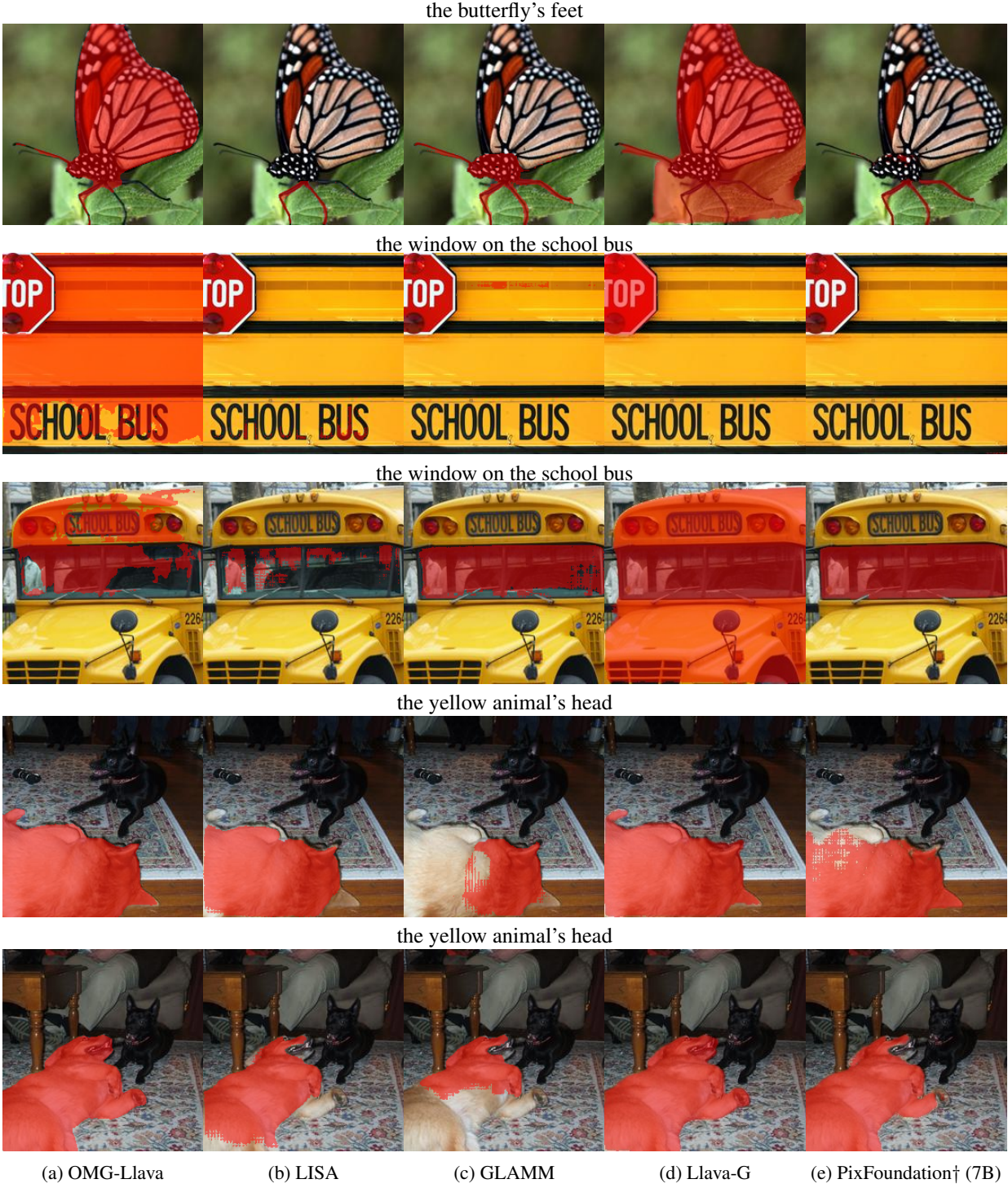


**Figure 18.** **PixMMVP** qualitative comparison between the pixel-level visual grounding following the second probing. The referred expression used in the segmentation is shown on top of each row. It shows persistently that mining for the grounding within attention maps of MLLMs that were not trained with pixel-level grounding supervision and using the oracle selection outperforms the pixel-level MLLMs. It clearly shows the oracle excels in identifying fine-grained object parts and descriptions that other pixel-level MLLMs are not necessarily capable of. The second best performance is GLAMM, yet we showed it is completely incapable of performing visual question answering unless fine-tuned for the region captioning task at which then it loses its grounding ability.



*Figure 19. PixCV-Bench* qualitative comparison between the pixel-level visual grounding following the second probing. The referred expression used in the segmentation is shown on top of each row. It shows similar to PixMMVP that mining for the grounding within MLLMs that were not trained with pixel-level grounding supervision paired with the oracle selection outperforms pixel-level MLLMs.

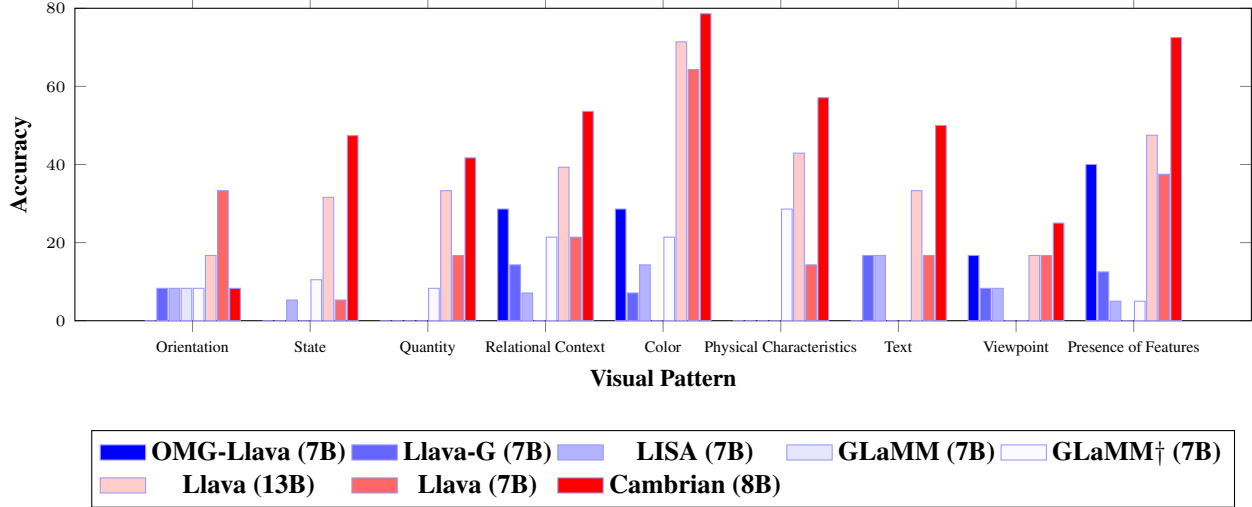


Figure 20. Fine-grained analysis of the studied models performance across the different visual pattern in PixMMVP showing the model’s accuracy with each pattern.

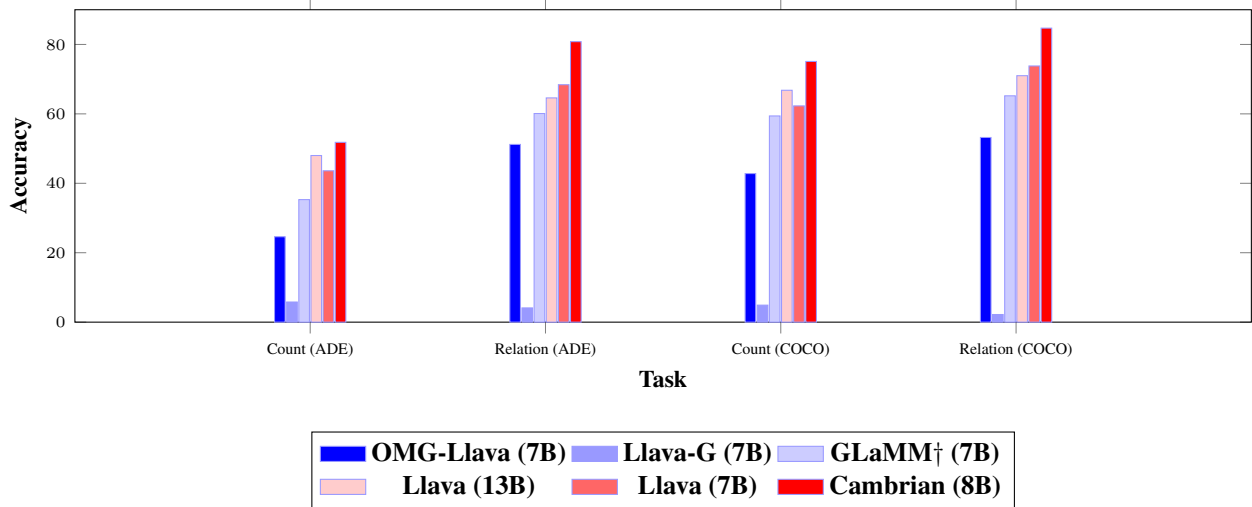
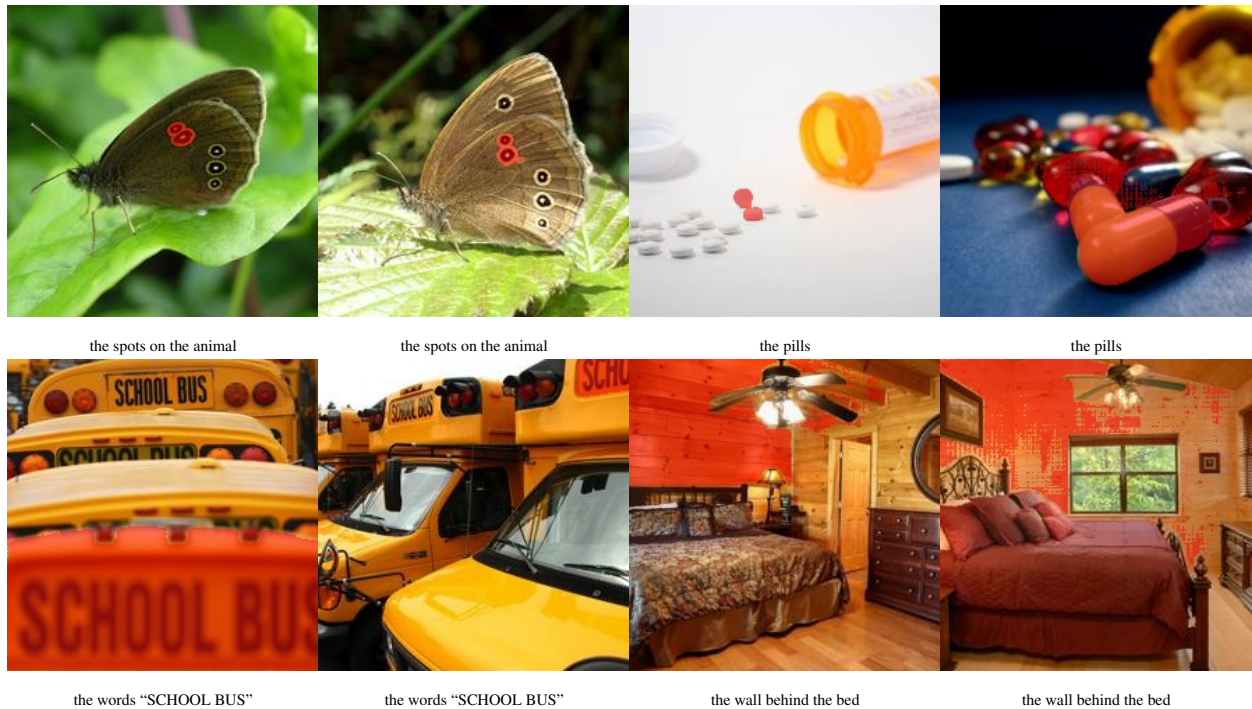


Figure 21. Fine-grained analysis of the studied models performance across the different visual patterns in PixCV-Bench (ADE20K and COCO), showing the model’s accuracy with each pattern.



*Figure 22.* Failures of the *oracle* upper bound, PixFoundation<sup>†</sup>, using Cambrian-1 (8B) as base MLLM on PixMMVP. It shows the failures mostly emerge in quantity or counting tasks. It also shows that the upper bound is inheriting SAM failures and the ambiguity arising in the referred expression itself, e.g., “the wall behind the bed”, which direction does “behind” indicate.